Journal of Materials Chemistry C

Accepted Manuscript

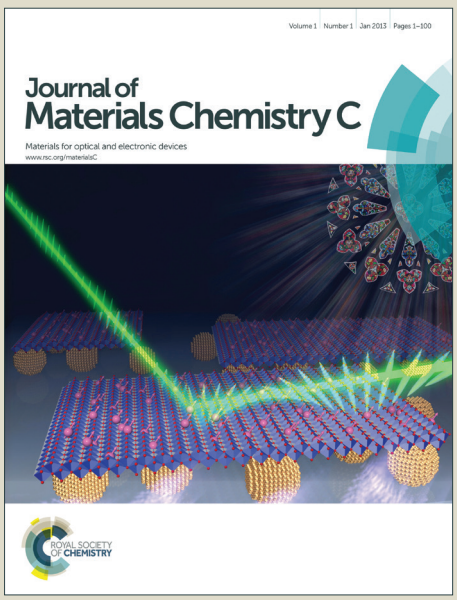

ROYAL SOCIETY OF CHEMISTRY

www.rsc.org/materialsC

Journal of Materials Chemistry RSCPublishing

ARTICLE

Flux-solvothermal preparation of dispersible $LiLa_{0.4}Nd_{0.6}(PO_3)_4$ microcrystals with regular morphology and superior fluorescence

Cite this: DOI: 10.1039/x0xx00000x

Received 00th January 2012,
Accepted 00th January 2012

DOI: 10.1039/x0xx00000x

www.rsc.org/

Zhongyue Wang, [a] Weikuan Duan, [a] Xiaoxia Cui, [c] Chen Liang, [b] Ruilin Zheng, [b] Wei Wei[bc*]

A flux-solvothermal method was firstly used to grow a kind of novel dispersible $LiLa_{0.4}Nd_{0.6}(PO_3)_4$ microcrystals with high Nd^{3+} ions concentration of 2.63×10^{21} cm^{-3} and excellent fluorescence properties for the first time. By optimizing experimental conditions, the microcrystals with the sizes in the region of 1.5~5 μm, strong emission intensity and long lifetime of 107 μs were obtained. The results show that their transparent dispersion in the mixed solvents of DMSO and $CHBr_2CHBr_2$ had strong absorption at 800 nm, low solvent quenching ratio of 6.5%, high quantum yield of 32.17% and large emission cross section of 4.39×10^{-20} cm^2 when Nd^{3+} ions concentration is 1×10^{20} cm^{-3}, which imply the microcrystals is of potential application in transparent glass-ceramics, dispersion amplifiers and lasers.

Introduction

Lithium-neodymium tetraphosphate [$LiNd(PO_3)_4$, LNP] crystal, as a result of its high Nd^{3+} ions concentration, strong absorption coefficient, low pump threshold and high conversion efficiency, is regard as an extraordinary promising miniature laser material. In LNP crystal, the Nd^{3+} ions concentration (N) can reach 4.39×10^{21} cm^{-3}, [1] which is approximately ca.32 times higher in commercial 1.0 at% Nd:YAG crystal. Although it has so high concentration of Nd^{3+} ions, the fluorescence quenching effect of LNP crystal is particularly weak duo to weakening of the dipole interaction between Nd^{3+} ions separated by the group of —O—P—O—.[2] Therefore, the fluorescence lifetime of LNP crystal still keeps special long under high Nd^{3+} concentration, and the cross relaxation rate (Q) is only about 0.5×10^{-43} cm^6, it is about 20 times smaller than that of Nd:YAG.[3] At the same time, the absorption cross section (σ_a) and emission cross section (σ_e) are equivalent to these of Nd:YAG while the lifetime (τ) is about half of that of Nd:YAG (**Table 1**). Then the gain coefficient of LNP crystal proportional to $\sigma_a\sigma_e\tau N$ [4] is about 20 times larger than that of Nd:YAG, all these imply that LNP crystal can obtain higher optical gain in short optical path. Up to now, LNP crystal has the lowest saturation parameter (I_s) of 49 Wmm^{-2} [3] and the lowest measured pump threshold energy of 0.14 mw. [5] Besides, LNP possesses no ferroelastic twinning domains and doesn't have the pronounced cleavability of NdP_5O_{14} (NPP). [6]

As a high quality laser material, LNP crystal was investigated in the early 1970s, but it hasn't been applied widely so far. One of the most important reasons is that large size of LNP crystal is too difficult to grow. In past 40 years, two methods, including high-temperature solution method [9-11] and flux method, [12-14] were used to grow LNP single crystal. Compared to high-temperature solution method, flux method has many outstanding advantages, such as wider applicability, simpler device, lower growing temperature and higher crystalline quality, so it become the main method for preparing LNP crystal. However, low growing temperature means slow growth rate and long growth cycle, and more importantly, it will cause small crystal size.

Table.1 The concentration of Nd^{3+} ions (N), absorption cross section (σ_a), absorption coefficient (α_p), emission cross section (σ_e) and fluorescence lifetime (τ) for Nd:YAG and LNP crystal

Crystal	Nd: YAG (1.0 at %)	LNP
$N(10^{20}\,cm^{-3})$	1.38	43.9
$\sigma_a(10^{-20}\,cm^2)$	12	12.5
$\alpha_p(cm^{-1})$	16.56	548.75
$\sigma_e(10^{-20}\,cm^2)$	28	32
$\tau(\mu s)$	230	120
$\sigma_a\sigma_e\tau N(10^{-15}\,cm\cdot\mu s)$	1.066	21.072
ref	7,8	1,3,4

Scientists had investigated the structure, morphology and optical properties of nanoparticles for many years, [15-17] and many people began to focus their attentions on neodymium ultraphosphate micro- and nano-crystals in past few years. *H.Naili* investigated the synthesis, structural, IR spectroscopy and conductivity of $AgGd(PO_3)_4$ powder in 2006, [18] and *T. Shalapska* studied the luminescence properties of Ce^{3+}-doped $LiGdP_4O_{12}$ microcrystals in 2009. [19] Since the growing temperature of melt solution technique was over 550 °C, it results in fast-growing of crystals and irregular morphology with the sizes in the region of 5~100 μm. Almost at the same

time, NdP_5O_{14}, $LiLnP_4O_{12}$ (Ln=La/Nd, Yb) [20-21] and $LiLn(PO_3)_4$ (Ln=La/Nd, Eu) [22-23]nanocrystals were reported. Yet the work by using flux method to make $LiNd(PO_3)_4$ microcrystals have never been reported.

In this paper, a flux-solvothermal method was utilized to prepare $LiLa_{0.4}Nd_6(PO_3)_4$ microcrystals. We investigated the influence of the preparation conditions containing growth temperature, growth time and solvothermal on its fluorescence intensity and lifetime at first. Under the optimal conditions, $LiLa_{0.4}Nd_{0.6}(PO_3)_4$ microcrystals have perfect crystallization with relatively small size of 1.5~5 μm. What's more, they can be dispersed in a mixed solvent of DMSO/$CHBr_2CHBr_2$ to form a transparent dispersion, and has particularly low solvent quenching rate. Besides, the emission quantum yield and the emission cross section of the dispersion with Nd^{3+} ions concentration of 1×10^{20} cm^{-3} were calculated as 32.17% and 4.39×10^{-20} cm^{-2} respectively based on the Judd-Ofelt theory.

Experimental

Materials

HNO_3 (GR, 65-68%), CH_3CH_2OH (AR) and H_3PO_4 (GR, ≥85%) were obtained from Aladdin Chemistry Co., Ltd. Urea while Li_2CO_3 (99%), Nd_2O_3(99.9%),La_2O_3 (99.9%),DMSO (99.9%) and $CHBr_2CHBr_2$ (97%) were provided by Alfa Aesar

Preparation of $LiLa_{0.4}Nd_{0.6}(PO_3)_4$ microcrystals

In a typical synthesis, 25 ml of phosphoric acid (85%) containing 0.6 mmol Nd_2O_3, 0.4 mmol La_2O_3, 8.5 mmol Li_2CO_3 were added to a 50 ml glassy carbon crucible under agitation. The reaction was controlled at 250 °C for 24 h to evaporate the free water first, then rise the temperature to 330 °C and keep it for 3h. Follow on, the crucible was cooled to room temperature in the air, and the product were washed by boiled water, 0.1 mol/L HNO_3, cold water and ethanol for 3 times orderly. The collected product was put in a 100 mL Teflon-lined autoclave with 70mL ethanol and treated at 180 °C for 12 h. After solvothermaltreament, the reactor was cooled to room temperature, and the products were centrifuged and washed by water and ethanol for 3 times. Finally, the residual precipitation was dried at 60 °C for 48 h at vacuum.

Preparation of $LiLa_{0.4}Nd_{0.6}(PO_3)_4$ microcrystals dispersion

The dispersion was prepared by adding 0.5 mL mixed solvents of DMSO and $CHBr_2CHBr_2$ under definite volume proportion in quartz cuvette containing 67 mg $LiLa_{0.4}Nd_{0.6}(PO_3)_4$ microcrystals powder and treated by ultrasonic finally.

Characterization

The fluorescence spectra of all $LiLa_{0.4}Nd_{0.6}(PO_3)_4$ samples were recorded by ZolixOmini-k 300 spectrophotometer pumped by a laser diode at 800 nm, and the luminescence decay times were measured by a 300 MHz Tektronix oscilloscope (Model 3032B). The quantum yield of $LiLa_{0.4}Nd_{0.6}(PO_3)_4$ microcrystals dispersion was tested on full-featured steady state/transient fluorescence spectrometer FLS920 from Edinburgh Instruments. The X-ray diffraction (XRD) patterns were measured on a Rigaku Dmax-2400 X-ray powder diffractometer with graphite monochromatized Cu Kα radiation (kα=0.2 nm). The morphologies were characterized by a JEOL JEM-2100F field emission transmission electron microscope (TEM) under a 200 kV working voltage. The transmissivity and absorption spectrum of dispersion were recorded using a UV-vis-NIR spectrophotometer (Shimadzu UV-3600) at room temperature.

Results and discussion

The fluorescence intensity and lifetime of as prepared $LiLa_{0.4}Nd_{0.6}(PO_3)_4$ microcrystals are mainly affected by growth temperature, growth time and solvothermal, which have been discussed in detail as follows.

Effect of growth temperature on fluorescence properties

It is well-known that growth temperature plays the leading role on growing crystals by flux method. Generally, phosphoric acid (H_3PO_4) will lose water into pyrophosphate ($H_4P_2O_7$) at about 250 °C, then turns into metaphosphate (HPO_3) at 280 °C, which is the cause of that flux method is often carried out at above 300 °C on growing LNP crystals. Therefore, three temperatures of 300 °C, 330 °C and 360 °C were chose as the growth temperature of $LiLa_{0.4}Nd_{0.6}(PO_3)_4$ microcrystals.

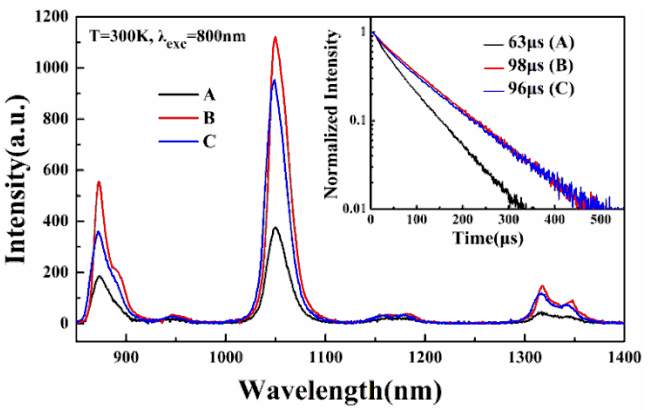

Fig.1 Fluorescence spectra of $LiLa_{0.4}Nd_{0.6}(PO_3)_4$ microcrystals prepared at (A)300 °C, (B)330 °C and (C)360 °C for 2 h. The inset is the fluorescence decay curves of corresponding samples.

Fig.1 is the fluorescence spectra and fluorescence decay curves of $LiLa_{0.4}Nd_{0.6}(PO_3)_4$ microcrystals prepared at different temperature for 2h. Obviously, three fluorescence spectra are consistent and the lifetimes are longer than $LaPO_4$: Nd (5 mol%) (90μs). [24] By increasing the growth temperature from 300 °C to 330 °C, the fluorescence intensity and lifetime improved markedly. The main reason is that higher temperature prolonged the effective growth time and quickened the growth rate. In fact, high temperature process of 2 h can be divided into two parts, including the water evaporation from $H_4P_2O_7$ to HPO_3 and the effective growth of $LiLa_{0.4}Nd_{0.6}(PO_3)_4$. Higher temperature will speed up the evaporation of water and

prolonged the effective growth time indirectly, as well as quickened the growth rate.

Nevertheless, higher temperature is not always better. On one hand, it will increase the number of nuclei and the range of particle distribution. On the other hand, exorbitant temperature often associated with a variety of crystal types and defect, which will affect the optical properties seriously. The weaken of fluorescence properties of $LiLa_{0.4}Nd_{0.6}(PO_3)_4$ is probably the main cause of crystal defects by further increasing the temperature from 330 °C to 360 °C.

Effect of growth time on fluorescence properties

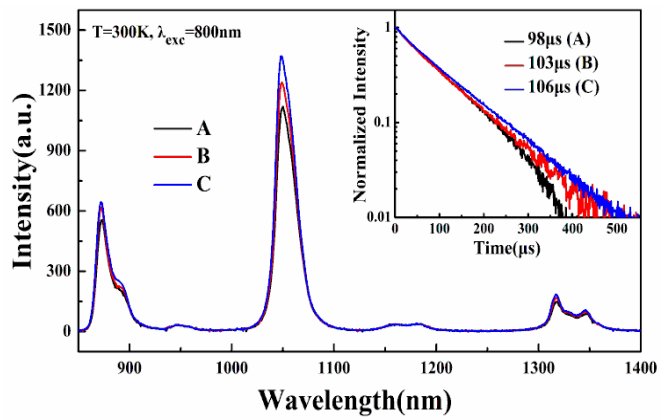

Fig.2 Fluorescence spectra of $LiLa_{0.4}Nd_{0.6}(PO_3)_4$ microcrystals prepared at 330 °C for (A)2 h, (B)4 h and (C)8 h. The inset is the fluorescence decay curves of corresponding samples.

In determining 330 °C as the optimal growth temperature, the influence of growth time on fluorescence spectra and fluorescence decay curves of $LiLa_{0.4}Nd_{0.6}(PO_3)_4$ microcrystals was shown in **Fig.2**.

By prolonging reaction time from 2 h to 8 h, both the fluorescence intensity and lifetime were improved to some extent, but the increase rate reduced gradually. It is well known that the specific surface area will reduce slowly while the size of the microcrystals increases rapidly with the extension of growth time. So the fluorescence performance will be proportional to the increases of effective active ions ratio caused by specific surface area decreasing, which can match the **Fig.2** very well. But, the fluorescence performance enhancement is limited in extending the growth time, and 4h was designated as the best growth time.

Effect of solvothermal treatment on fluorescence properties

As a broad synthesis method of inorganic semiconducting nanostructures, [25] hydrothermal treatment is not only an effective approach on optimizing the crystallization for more complete, but also a way to remove impurities to a certain degree. Herein we added a solvothermal process to expect better fluorescence performance. As it can be seen from the fluorescence spectra and fluorescence decay curves of $LiLa_{0.4}Nd_{0.6}(PO_3)_4$ microcrystals by different treatments (**Fig.3**), the fluorescence properties of the microcrystals treated at 180 °C for 12 h in ethanol were improved markedly, which was roughly correspondent with our wishes.

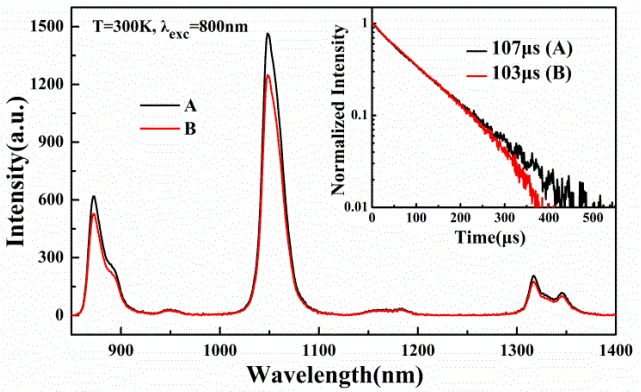

Fig.3 Fluorescence spectra of $LiLa_{0.4}Nd_{0.6}(PO_3)_4$ microcrystals prepared at 330 °C for 4 h following by (A) solvothermal treatment at 180 °C for 12 h and (B)without solvothermal treatment. The inset is the fluorescence decay curves of corresponding samples.

Morphology and crystal phase of $LiLa_{0.4}Nd_{0.6}(PO_3)_4$ microcrystals

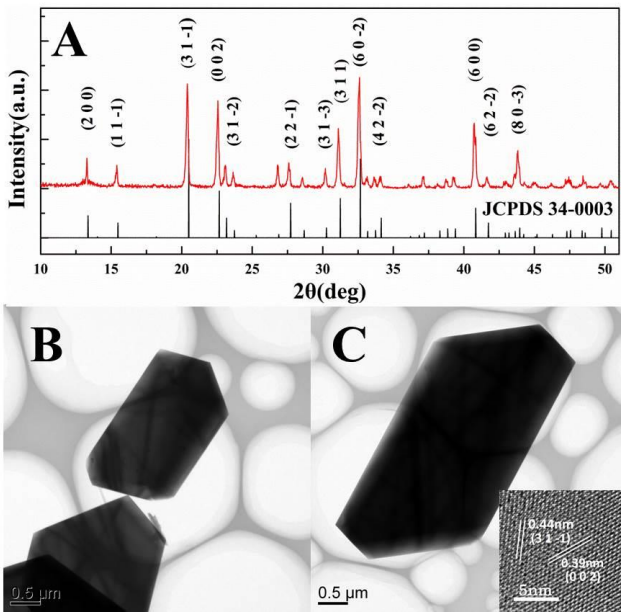

Fig.4 XRD patterns (A) and TEM images (B and C) of $LiLa_{0.4}Nd_{0.6}(PO_3)_4$ microcrystals prepared at 330 °C for 4h, following by solvothermal treatment at 180 °C for 12 h. The inset is HRTEM of $LiLa_{0.4}Nd_{0.6}(PO_3)_4$ microcrystals.

By the optimal experimental conditions, $LiLa_{0.4}Nd_{0.6}(PO_3)_4$ microcrystals with perfect crystallization and relatively small size were obtained, as shown in **Fig.4**. All the diffraction peaks can match with the standard card (JCPDS 34-0003) perfectly **(Fig.4A),** which means the product crystallizes in pure monoclinic-phase of $LiNd(PO_3)_4$. The sharp diffraction peaks illustrated that the size of $LiLa_{0.4}Nd_{0.6}(PO_3)_4$ is a little big, it was proved by the TEM images of the microcrystals, which had regular shape and a size range of 1.5~5 μm (**Fig.4B** and **C**). Besides, HRTEM (the inset of Fig.4C) reveal that these

microcrystals are single-crystalline, and they mainly show the lattice fringes of (3 1 -1) plane and (0 0 2) plane.

As everyone knows, an oblique crystal surface is the biggest feature of monoclinic system. All the $LiLa_{0.4}Nd_{0.6}(PO_3)_4$ microcrystals observed in the TEM images have oblique crystal surface, illustrating that the microcrystals crystallized in monoclinic-phase. What's more, all the angles signed in the TEM image are about 126 °, consistent with the cell parameters (β=126.46°) of $LiNd(PO_3)_4$,[1] which is another evidence of monoclinic $LiLa_{0.4}Nd_{0.6}(PO_3)_4$ microcrystals.

Optical properties of $LiLa_{0.4}Nd_{0.6}(PO_3)_4$ microcrystals dispersion

A noteworthy phenomenon is that $LiLa_{0.4}Nd_{0.6}(PO_3)_4$ microcrystals can be dispersed in a mixed solvents of DMSO and $CHBr_2CHBr_2$ in a certain volume ratio to form a transparent purple dispersion (the inset of **Fig.5**). Generally, the scattering phenomenon of particles dispersion will rise sharply with increasing the particles size, embodying in serious muddy performance of the dispersion.

Besides, another factor affected the transmittance of the dispersion is the matching degree of refractive index between particles and solvents. [26] In view of the particles of $LiLa_{0.4}Nd_{0.6}(PO_3)_4$ in micron level, we identified that adjusting the refractive index of solvents to match that of $LiLa_{0.4}Nd_{0.6}(PO_3)_4$ microcrystals is the only way to get a transparent dispersion. Finally, $CHBr_2CHBr_2$ and DMSO were chose as the main solvent.

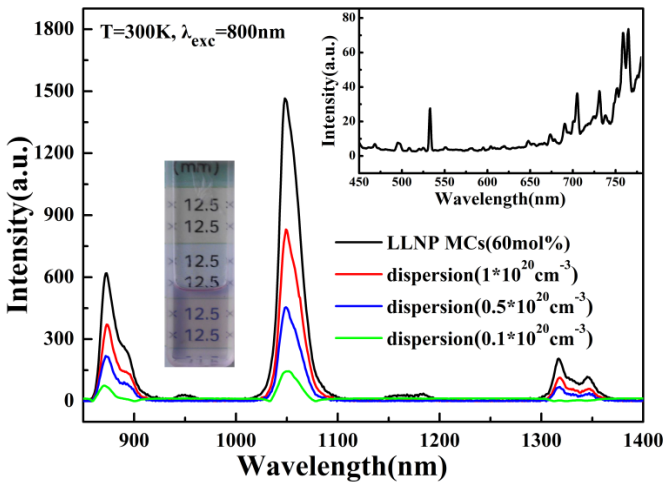

Fig.5 Fluorescence spectra of $LiLa_{0.4}Nd_{0.6}(PO_3)_4$ microcrystals and their dispersions in DMSO/$CHBr_2CHBr_2$ with different Nd^{3+} ions concentrations. The inset is the photograph of $LiLa_{0.4}Nd_{0.6}(PO_3)_4$ microcrystals dispersion with Nd^{3+} ions concentration of 1×10^{20} cm^{-3} in quartz utensil (2 mm×10 mm×45 mm) and upconversion spectrum.

Fig.5 is the fluorescence spectra of $LiLa_{0.4}Nd_{0.6}(PO_3)_4$ microcrystals and their dispersions in DMSO/$CHBr_2CHBr_2$ with different Nd^{3+} ions concentrations. Unlike $LiLa_{1-x}Nd_xP_4O_{12}$ nanocrystals, [27] no upconversion phenomenon was observed, as shown in the inset of **Fig.5**. Along with the increase of the dispersion concentration, the fluorescence intensity enhance correspondingly, and overtook half of that of $LiLa_{0.4}Nd_{0.6}(PO_3)_4$ microcrystals at Nd^{3+} ions concentration of 1×10^{20} cm^{-3}. Besides, the fluorescence intensity decreased by 376 when the Nd^{3+} ions concentration reduced from 1×10^{20} cm^{-3} to 0.5×10^{20} cm^{-3}, and weakened by 686 as the concentration decreased from 1×10^{20} $cm^{-3}$to 0.1×10^{20} cm^{-3}. Similar decay rates of fluorescence intensity to Nd^{3+} ions concentration (7.52×10^{-18} cm^3 and 7.62×10^{-18} cm^3) illustrated that the quenching effect of mixed solvent on $LiLa_{0.4}Nd_{0.6}(PO_3)_4$ microcrystals is extremely weak. Hence, we surmised that the fluorescence lifetime would fluctuate weakly as decreasing the Nd^{3+} ions concentration of dispersion.

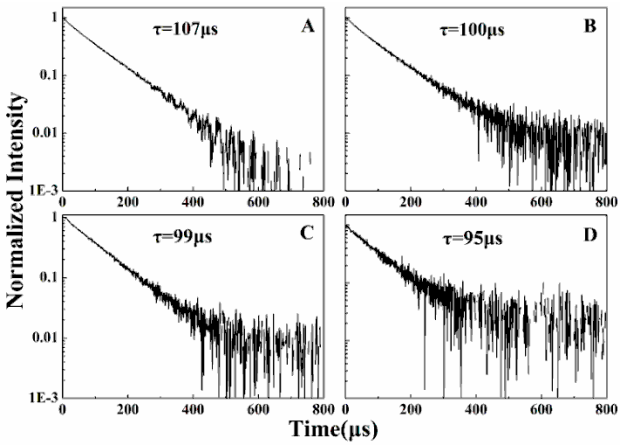

Fig.6 Fluorescence decay curves of $LiLa_{0.4}Nd_{0.6}(PO_3)_4$ microcrystals (A) and their dispersions in DMSO/$CHBr_2CHBr_2$ with different Nd^{3+} ions concentrations: (B)1×10^{20} cm^{-3}, (C)0.5×10^{20} cm^{-3} and (D)0.1×10^{20} cm^{-3}.

By fitting the fluorescence decay curves of $LiLa_{0.4}Nd_{0.6}(PO_3)_4$ microcrystals and their dispersions with different Nd^{3+} ions concentrations (**Fig.6**) by using single exponential function, four lifetimes of 107 μs, 100 μs, 99 μs and 95 μs were obtained respectively. Based on the equation of $(\tau_{powder}-\tau_{dispersion})/\tau_{powder}$, particular low quenching rates of solvents on $LiLa_{0.4}Nd_{0.6}(PO_3)_4$ microcrystals were calculated as 6.54%, 7.48% and 11.2% for three kinds of Nd^{3+} ions concentrations, which confirmed above conjecture.

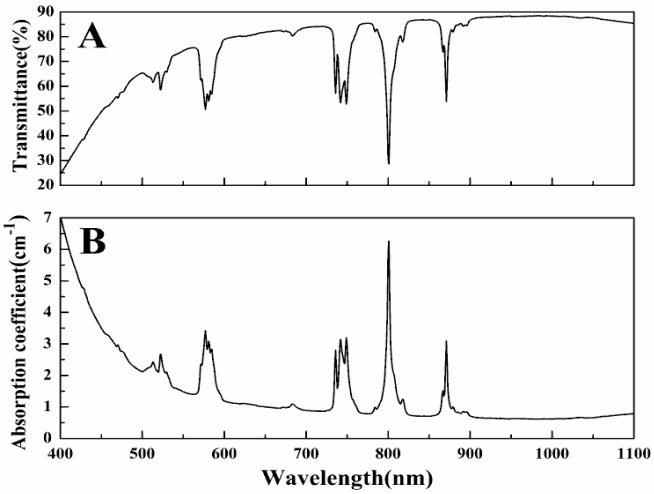

Fig.7 Transmittance(A) and Absorption coefficient (B) spectra of $LiLa_{0.4}Nd_{0.6}(PO_3)_4$ microcrystals dispersion with Nd^{3+} ions concentration of 1×10^{20} cm^{-3}.

In addition, the transmittance and absorption coefficient spectra of $LiLa_{0.4}Nd_{0.6}(PO_3)_4$ microcrystals dispersion with Nd^{3+} ions concentration of 1×10^{20} cm^{-3} were measured (**Fig.7**). Five absorption peaks can be observed obviously, and the special sharp peak at 800 nm means strong absorption of the excitation light, which can be seen in **Fig.7B**. However, the transmittance of the dispersion was very low in the visible region below 550 nm, which is mainly caused by scattering of relatively large particles size.

Judd-Ofelt analysis

According to the Judd-Ofelt theory and the absorption coefficient spectrum of $LiLa_{0.4}Nd_{0.6}(PO_3)_4$ microcrystals dispersion (**Fig.7B**), some optical paremeters were calculated to evaluate the laser performance of the dispersion. Under reference to the refractive index of LNP single crystal, [28] five experimental oscillator strengths (f_{exp}) of electronic transitions of Nd^{3+} ions from ground state ($^4I_{9/2}$) to various excited states can be calculated by Equation 1.

$$f_{\exp} = \frac{mc^2}{\pi e^2 N\lambda^2}\int \alpha(\lambda)d\lambda \qquad (1)$$

Where *m* and *e* are electron mass and charge, *c* is the velocity of light, *N* is the number density of Nd^{3+} ions, and α (λ) is the absorption coefficient.

Based on Equation 2, the calculated oscillator strengths (f_{cal}) of electronic transitions from the ground state (*aJ*) level to the excited state (*bJ′*) level are obtained.

$$f_{cal}(aJ,bJ') = \frac{8\pi^2 mc\chi}{3h\lambda(2J+1)}S \qquad (2)$$

Where χ is the local field correction factor expressed as $\chi=n(n^2+2)^2/9$, *h* is the Planck constant, $2J+1$ is the degeneracy of the ground state, and *S* is the spectral line intensity of the electronic dipole transitions, which can be expressed as the following equation:

$$S = \sum_{t=2,4,6}\Omega_t\left|\left\langle aJ\left\|U^{(t)}\right\|bJ'\right\rangle\right|^2 \qquad (3)$$

Here $|\langle aJ\|U(t)\|bJ'\rangle|^2$ represents the reduced matrix elements given by *Carnall* et al. [29] The J-O parameters $\Omega_{t(2,\,4,\,6)}$ are calculated by a least-squares fitting of f_{exp} to f_{cal}.

The absorption bands, absorption coefficient, experimental and theoretical oscillator strengths and Judd-Ofelt parameters $\Omega_{t\ (2,\,4,\,6)}$ obtained for LNP nanocrystals dispersion with Nd^{3+} ions concentration 1×10^{20} cm^{-3} were presented in **Table.2**.

On the basis of $\Omega_{t\ (2,\,4,\,6)}$ parameters, the emission line strengths corresponding to transitions from the upper multiplet manifolds $^{2S+1}L_J$ to the lower manifolds $^{2S'+1}L'_{J'}$ can be calculated.

$$S_{ed}(J,J') = \frac{3hc(2J+1)}{8N\pi^3 e^2\lambda}\frac{1}{\chi}\int k(\lambda)d\lambda \qquad (4)$$

Table.2 Observed absorption peak positions, integrated absorption coefficient, measured oscillator strengths (f_{exp}), calculated oscillator strengths (f_{cal}) and Judd-Ofelt parameters of $LiLa_{0.4}Nd_{0.6}(PO_3)_4$ microcrystals dispersion.

Transition $^4I_{9/2}\rightarrow$	Absorption peak (nm)	Absorption coefficient $\int\alpha(\lambda)d\lambda$ (10^{-7})	Oscillator strength f_{exp} (10^{-6} cm^2)	Oscillator strength f_{cal} (10^{-6} cm^2)
$^4G_{7/2}+^4G_{9/2}+^2K_{13/2}$	522	10.93717	3.18898	5.16737
$^4G_{5/2}+^2G_{7/2}$	577	30.15092	7.19509	10.1946
$^4F_{7/2}+^4S_{3/2}$	748	36.19294	5.13935	7.48703
$^4F_{5/2}+^4H_{9/2}$	800	43.77406	5.4205	7.39324
$^4F_{3/2}$	871	16.66125	1.74485	2.45756
Ω_2 ($\times10^{-20}$$cm^2$)		0.6215		
Ω_4 ($\times10^{-20}$$cm^2$)		4.8187		
Ω_6 ($\times10^{-20}$$cm^2$)		5.1725		

Then the radiative decay rates *A* (*J*→*J′*) for transitions between the upper manifold (*J*) and the corresponding lower-lying multiplet manifolds (*J′*) is obtained by the following expression.

$$A(J\rightarrow J') = \frac{64\pi^4 e^2\chi}{3h(2J+1)\lambda^3}S_{ed}(J\rightarrow J') \qquad (5)$$

The radiative lifetime τ_r of the excited state $^4F_{3/2}$ (*J*=3/2) is calculated through following Equation.

$$\tau_r = \frac{1}{A_{ed}} = \frac{1}{\sum A(J\rightarrow J')} \qquad (6)$$

The fluorescence branching ratios β (*J*→*J′*) for transitions originating from the $^4F_{3/2}$ manifold are determined from the radiative decay rates by Equation 7.

$$\beta(J\rightarrow J') = A(J\rightarrow J')\tau_r \qquad (7)$$

The quantum efficiency (φ) of the emission bands can be evaluated from function 8.

$$\varphi = \frac{\tau_{mea}}{\tau_{rad}} \qquad (8)$$

Besides, the stimulated emission cross section (σ) for $^4F_{3/2}\rightarrow{}^4I_{11}/_2$ transition is calculated by Equation (9).

$$\sigma = \frac{\lambda_p^4}{8\pi n_d^2 c}\frac{1}{\Delta\lambda_{eff}}A_{ed}(a,b) \qquad (9)$$

Where $\Delta\lambda_{eff}$ is the effective fluorescence line width at the peak wavelength (λ_p) for $^4F_{3/2}\rightarrow{}^4I_{11}/_2$ transition and is equal to

$$\Delta\lambda_{eff} = \frac{\int I(\lambda)d\lambda}{I_{max}} \qquad (10)$$

The radiative decay rates (A_{rad}), fluorescence branching ratios (β_{exp}), radiative lifetime (τ_r) of the excited state $^4F_{3/2}$ (*J*=3/2), quantum yield and emission cross section of the $^4F_{3/2}\rightarrow{}^4I_{11/2}$ were listed in **Table.3**.

Table.3 Observed emission bands, their measured and calculated radiative properties of $LiLa_{0.4}Nd_{0.6}(PO_3)_4$ microcrystals dispersion.

$^4F_{3/2}$ →	Wavelength (nm)	A_{rad} (s^{-1})	β_{exp} (%)	τ_{cal} (μs)	η (%)	σ (10^{-20} cm^2)
$^4F_{9/2}$	871	1358.24	42.22			
$^4I_{11/2}$	1049	1551.44	48.22	311	32.17	4.39
$^4I_{13/2}$	1318	307.49	9.56			

Finally, a high quantum efficiency of 32.17% and large emission cross section of $4.39*10^{-20}$ cm^2 for $LiLa_{0.4}Nd_{0.6}(PO_3)_4$ microcrystals dispersion were obtained. The radiative lifetime calculated for dispersion was 311 μs, which is in close proximity to the lifetime of $LiLa_{1-x}Nd_x(PO_3)_4$ (x=0.01) nanocrystals (354 μs) we measured [30] and the radiative lifetime of LNP nanocrystals dispersion (321 μs). Then the emission quantum yield reached a high value of 32.17%.

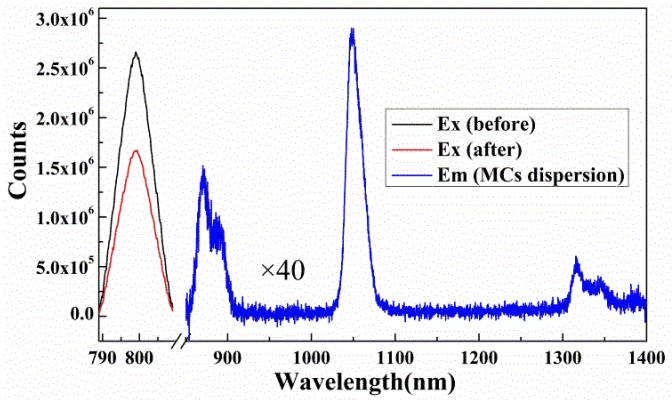

Fig.8 Excitation light and fluorescence spectra of $LiLa_{0.4}Nd_{0.6}(PO_3)_4$ microcrystals dispersion in DMSO/$CHBr_2CHBr_2$.

In order to validate the reliability of quantum yield we calculated, a test quantum yield of $LiLa_{0.4}Nd_{0.6}(PO_3)_4$ microcrystals dispersion in DMSO/$CHBr_2CHBr_2$ was taken, as shown in **Fig.8**. By integrating the emission intensity and excitation intensity, we can obtained the photon counts emitted and absorbed by $LiLa_{0.4}Nd_{0.6}(PO_3)_4$ microcrystals dispersion. Then the test quantum yield, the quotient of emitted photon counts divided by absorbed photon counts, was determined to be 35.51%, which is a little higher than the value by Judd-Ofelt calculation.

Conclusions

In summary, $LiLa_{0.4}Nd_{0.6}(PO_3)_4$ microcrystals with the sizes of 1.5~5 μm were grown via flux-solvothermal method by optimizing growth temperature and time, and solvothermal process. They can be dispersed in mixed solvents of DMSO and $CHBr_2CHBr_2$ to form a transparent purple dispersion, which had high quantum yield of 32.17%, large emission cross section of 4.39×10^{-20} cm^2 and low quenching ratio of 6.5%. It is a potential gain medium for transparent glass-ceramics, dispersion amplifiers and lasers.

Acknowledgements

This work was financially supported by the National Basic Research Program of China (No. 2012CB933301) and National Natural Science Foundation of China (No.60977023, 61077070, 61107015 and 61177086).

Notes and references

[a]Institute of Advanced Materials (IAM), NanjingUniversity of Posts andTelecommunications (NUPT), Nanjing 210023, P.R. China.
[b]School of Optoelectronic Engineering, Nanjing University of Posts andTelecommunications (NUPT), Nanjing 210023, P.R. China. E-mail: iamww@fudan.edu.cn
[c]State Key Laboratory of Transient Optics and Photonics, Xi'an Institute of Optics and precision Mechanics, Chinese Academy of Science (CAS), Xi'an 710119, P. R. China.

1. H. Ettis, H. Na ïi and T. Mhiri,*J. Solid State Chem*., 2006, **179**, 3107.
2. J. Zhu, W.D. Cheng, D.S. Wu,H. Zhang, Y.J. Gong, H.N. Tong, D. Zhao, *Eur. J. Inorg. Chem*., 2007, **2007**, 285.
3. K. Otsuka, T. Yamada, M. Saruwatari, T. Kimura,*IEEE. J. QE*., 1975, **QE-11**, 330.
4. K.Otsuka and T. Yamada, Proceedings of the IEEE. 1975, 63, 1621.
5. M. Saruwatari, T. Kimura and K. Otsuka,*Appl. Phys. Lett*., 1976, **29**, 291.
6. W.W. Kruhler, R.D. Plattner and W. Stetter,*Appl. Phys.*, 1979, **20**, 329.
7. T. Kushida, H. Marcos and J. Geusic,*Phys. Rev*., 1968, **167**, 289.
8. J. Lu, M. Prabhu, J. Song, C. Li, J. Xu, K. Ueda, A.A. Kaminskii, H. Yagi and T. Yanagitani,*Appl. Phys. B: Lasers O*., 2000, **71**, 469.
9. I. Oarreu, R. Sole, Jna. Gavalda, J. Massons, F. Diaz and M. Aguilo,*Chem. Mater*., 2003, **15**, 5059.
10. M. Fang, W. D. Cheng, Z. Xie, H. Zhang, D. Zhao, W.L. Zhang and S.L. Yang,*J. Mol. Struct.*, 2008. **891**, 25.
11. D. Zhao, H. Zhang, S.P. Huang, M. Fang, W.L. Zhang, S.L. Yang and W.D. Cheng,*J. Mol. Struct*., 2008, **892**, 8.
12. N.E. Ter-Gabrielyan, V.M. Markushev, V.R. Belan, Ch.M. Briskina, O.V. Dimitrova, V.F. Zolin and A.V. Lavin,*Sov. J. QE*., 1991, **21**, 840.
13. E.B. Zarkouna, M. F érid and A. Driss, *Mater. Res. Bull*., 2005, **40**, 1985.
14. K. Horchani-Naifer, J. Amami and M. Ferid, *J. Rare. Earth*., 2008, **26**,765.
15. F. Wang, Y. Han, C.S. Lim, Y.H. Lu, J. Wang, J. Xu, H.Y. Chen, C. Zhang, M.H. Hong, X.G. Liu. *Nature*., 2010, **463**, 1061.
16. X.C Ye, J. Chen, M. Engel, J.A. Millan, W.B. Li, L. Qi, G.Z. Xing, J.E. Collins, C.R. Kagan, J. Li, S.C. Glotzer, C.B. Murray. *Nat. Chem*., 2013, **5**, 466.
17. X.C. Ye, J.E. Collins, Y.J. Kang, J. Chen, D.T.N. Chen, A.G. Yodh, C.B. Murray. *PNAS*., 2010, **107**, 22430.
18. H. Na ïi, H. Ettis and T. Mhiri. *J. Alloy. Compd.* 2006, **424**, 400.
19. T. Shalapska, G. Stryganyuk, P. Demchenko, A. Voloshinovskii and P. Dorenbos, *J. Phys-Condens. Mat*., 2009. **21**, 445901.
20. M.Y. Sharonov, T. Myint, A. B. Bykov, V. Petricevic and R.R. Alfano, *J. Opt. Soc. Am. B*., 2007, **24**, 2868.
21. W. Strek, L. Marciniak, A. Bednarkiewicz, A. Lukowiak, R. Wiglusz and D. Hreniak, *Opt. Express*., 2011, **19**, 14083.

22. W. Strek, L. Marciniak, A. Lukowiak, A. Bednarkiewicz, D. Hreniak and R. Wiglusz, *Opt. Mater*., 2010, **33**, 131.
23. R.J. Wiglusz, R. Pazik, A. Lukowiak and W Strek, *Inorg. Chem*., 2011, **50**, 1321.
24. J.W. Stouwdam, G.A. Hebbink, J. Huskens and F.C.J.M. van Veggel, *Chem. Mater*., 2003, **15**, 4604.
25. W.D. Shi, S.Y. Song and H.J. Zhang, *Chem. Soc. Rev*., 2013, **42**, 5714.
26. W.X. Sun, X.X. Cui, Z.Y. Wang, W. Wei and B. Peng, *J. Mater. Chem*., 2012, **22**, 6990.
27. L. Marciniak, W.Strek, A.Bednarkiewicz, A. Lukowiak and D. Hreniak, *Opt. Mater*., 2011, **33**, 1492
28. J. Nakano, *J. Appl. Phys*., 1981, **52**, 1239.
29. W. T. Carnall, P. R. Fields and B. G. Wybourne, *J. Chem. Phys.*, 1968, **42**, 3797.
30. Z.Y. Wang, X.X. Cui, R.L. Zheng, W.K. Duan, B. Peng and W. Wei, *Nanoscale*., 2013, **5**, 10203.